Int. J. Heat Mass Transfer. Vol. 26, No. 4, pp. 607–619, 1983
Printed in Great Britain

0017–9310/83/040607–13 $03.00/0

GENERALIZED CORRELATION OF THE WATER FROST THERMAL CONDUCTIVITY

MARK A. DIETENBERGER
The University of Dayton Research Institute, 300 College Park, Dayton, OH 45469, U.S.A.

(*Received* 30 *September* 1981 *and in revised form* 13 *August* 1982)

Abstract—In recent years the study of frost formation has gained renewed emphasis. Crucial to the development of the frost formation model has been the derivation of the frost thermal conductivity, which is the subject of this paper. The thermal conductivity of the frost layer plays an important part in its structure and rate of formation. A number of published papers have addressed the problem of computing the frost thermal conductivity. In this paper, the various approaches used in these published papers are examined by analyzing the underlying assumptions of each treatment. Full understanding of these assumptions begins with a discussion of all possible heat transfer processes within the frost layer, to determine which processes are significant and which can be safely neglected. From this perspective, the different approaches taken in the published papers can be evaluated and the results can be compared with experimental data. Furthermore, the range of environmental conditions can be determined for which a particular approach is realistic and the limitations of each approach can then be deduced. It will be shown that none of the approaches are sufficient for a general frost model. As a result, a new, more comprehensive method of calculating the frost thermal conductivity based on both theory and experimental data has been developed.

NOMENCLATURE

a, $k_{\text{eff air}}/k_i$;
B, frost porosity, $(\rho_i-\rho_f)/(\rho_i-\rho_a)$;
B_c, proportion of the frost volume representing ice spheres and ice planes;
B_1, $0.1726\,(T/273.16)$;
B_2, 0.751;
B_3, $B_2+0.3$;
b, linear dimension of ice crystals;
C_p, effective specific heat of forced air flow in frost layer [J g^{-1} °C^{-1}];
D, ordinary diffusion coefficient fitted to data (ref. [9]), $1.198\times10^{-5}\,T^{1.75}\,(P_{atm}/P)$;
G_a, air mass flow rate per unit area [g m^{-2} s^{-1}];
K, thermal conductivity of frost [W m^{-1} °C^{-1}];
$\bar{K}$, average frost thermal conductivity [W m^{-1} °C^{-1}];
k_a, thermal conductivity of air [W m^{-1} °C^{-1}];
k_e, effective thermal conductivity of the combined heat conductive proportions of air and ice [W m^{-1} °C^{-1}];
k_i, thermal conductivity of ice [W m^{-1} °C^{-1}];
k_r, radiation thermal conductivity within the frost layer based on the Stefan–Boltzmann law and a geometric view factor [W m^{-1} °C^{-1}];
k_v, water vapor thermal conductivity [W m^{-1} °C^{-1}];
L, L_e or L_s;
L_e, latent heat of water evaporation [J g^{-1}];
L_s, latent heat of ice sublimination [J g^{-1}];
$\dot{m}_d$, water vapor mass flux within the frost layer [g m^{-2} s^{-1}];
$\dot{m}_{d_s}$, water flux driven by the temperature gradient at the frost surface [g m^{-2} s^{-1}];
$\dot{m}_{exp}$, experimentally calculated value of the water mass flux into the frost surface from the surrounding air [g m^{-2} s^{-1}];
$\dot{m}_t$, total water mass flux [g m^{-2} s^{-1}];
P_t, ambient pressure [N m^{-2}];
P_v, water vapor pressure [N m^{-2}];
P_v^*, pressure reference value, 610.7 N m^{-2};
q_0, constant heat flux at the wall [W m^{-2}];
R, saturation ratio;
R_v, water vapor gas constant, 0.4615 J g^{-1} K^{-1};
T, frost temperature [K];
T_s, frost surface temperature [K];
T_w, wall temperature [K];
T^*, temperature reference value, 273 K;
w_a, free stream humidity;
w_w, humidity at the wall temperature;
x, distance from the wall [m];
x_s, frost thickness [m].

Greek symbols

ε, emissivity, 0.985;
Θ, fractional volume of ice fragments, $(\rho_f-\rho_a)/(\rho_i-\rho_a)$;
ρ_f, frost density [g cm^{-3}];
ρ_v, saturated water vapor density [g cm^{-3}];
σ, Stefan–Boltzmann constant, 0.56697×10^{-7} W m^{-2} °C^{-4};
τ_s, tortuosity;
χ, relative concentration of water vapor [mol H_2O/mol air].

1. INTRODUCTION

IN RECENT years the study of frost formation has gained renewed emphasis. In particular, nocturnal frost on

aircraft wings has been known to cause aerodynamic penalties of lift and drag upon take-off. Present Federal Aviation Agency (FAA) regulations require frost removal on transport planes prior to take-off. This is usually done with expensive petroleum solvent. Meanwhile, general aviation aircraft take-off at their own risk because of less stringent FAA regulations. The accurate calculation of frost growth on the airfoil and the corresponding aerodynamic penalties required the development of a frost formation model much more complex than those available in the literature. Additional need for a sophisticated frost formation model relates to cryogenic technology. There is, for example, concern that frost will form on the external tank of the space shuttle. If enough frost forms on the tank, the probability exists that frost will shed during lift-off and damage the tiles on the space shuttle. An accurate frost formation model, instead of overly conservative assumptions about the frost layer on the tank, may allow one to maintain a round-the-clock launch schedule.

Crucial to the development of the frost formation model has been the derivation of the frost thermal conductivity, which is the subject of this paper. The thermal conductivity of the frost layer plays an important part in its structure and rate of formation. A number of published papers have addressed the problem of computing the frost thermal conductivity. In this paper, the various approaches used in these published papers are examined by analyzing the underlying assumptions of each treatment. Full understanding of these assumptions begins with a discussion of all possible heat transfer processes within the frost layer, to determine which processes are significant and which can be safely neglected. From this perspective, the different approaches taken in the published papers can be evaluated and the results can be compared with experimental data. Furthermore, the range of environmental conditions can be determined for which a particular approach is realistic and the limitations of each approach can then be deduced. It will be shown that none of the approaches are sufficient for a general frost model. As a result, a new, more comprehensive method of calculating the frost thermal conductivity based on both theory and experimental data has been developed.

2. THE HEAT TRANSFER PROCESSES WITHIN THE FROST LAYER

The various approaches to modeling of the frost temperature distribution and thus also the frost thermal conductivity can be derived from expressing the significant heat transfer processes within the frost layer by the energy equation

$$\frac{\mathrm{d}}{\mathrm{d}x}(k_e + k_r)\frac{\mathrm{d}T}{\mathrm{d}x} = -L\frac{\mathrm{d}\dot{m}_d}{\mathrm{d}x} - G_a C_p \frac{\mathrm{d}T}{\mathrm{d}x}. \quad (1)$$

Simplified from equation (37) in ref. [1], the following two assumptions were made. The first assumption is that within the frost layer, the temperature and the pressure are in a quasi-steady state. The energy storage rate will be important for nocturnal frost formation cases but for the cold wall cases considered in this report it is not important in analyzing the frost thermal conductivity. White [1] has shown that the temperature and the pressure in the frost layer are at most slowly varying functions of time, partly due to the isothermal conditions of the wall and because the frost surface temperature is near the melting point. The energy storage rate is then small compared with the heat flux; providing justification for the assumption of quasi-steady state. The second assumption is that the heat conduction and the black body radiation as given by the first two terms of equation (1) are 1-dim. (i.e. through the thin frost layer to the wall) for the purposes of comparing to experimental data on a flat plate. The 1-dim. internal heat generation rate produced by the phase change and the 1-dim. enthalpy change produced by air ventilation flow through the frost structure are given by the terms on the RHS of equation (1).

An analysis of the above energy equation by order of magnitude calculations is needed to determine the relative significance of each term. Specifically, four factors, k_e, k_r, $\dot{m}_d$ and G_a, will be investigated in the above equation. It will be demonstrated that the heat flux represented by the radiation k_r and the forced air enthalpy transport G_a are negligible in comparison to the thermal conductivity of the air–ice structure k_e and the latent heat release of the water vapor.

2.1. *Argument for significance of air–ice thermal conductivity, k_e*

Since the frost contains air and the crystals of ice, the conductivity of frost should be somewhere between the thermal conductivities of air and ice. The thermal conductivity of air is given by [2]

$$k_a = 2.646 \times 10^{-3}\left[\frac{T^{1.5}}{1+(245/T)10^{-12/T}}\right] \quad (2)$$

and that of ice by [3]

$$k_i = 630/T. \quad (3)$$

Thus k_e has been modeled in terms of the weighted functional relationship between the thermal conductivities of air and ice based on the density and the structure of the frost. Biguria and Wenzel [4] have compiled several theoretical models to formulate k_e based on various assumptions for the frost structure. The effective thermal conductivity models described by Biguria and Wenzel are based upon:

(1) Resistance in series for minimum possible conductivity (i.e. ice planes).

(2) Resistances in parallel for maximum possible conductivity (i.e. ice cylinders).

(3) Russel equation for porous media where the solid (ice) is in a continuous structure and there is a distribution of cubical pores arranged in a simple cubic lattice.

(4) Maxwell–Rayleigh equation for the case of fluid pores (air) distributed in a continuous solid (ice).

(5) Maxwell–Rayleigh equation for the case of solid pores (ice) distributed in a continuous fluid (air).

(6) The Brailsford–Major equation for the case when one phase of the constituents (say ice or air) is not spatially continuous.

(7) The Woodside equation for a cubic lattice of uniform solid spherical particles (ice) in a gas (air).

However, in the observations of frost formation, by Brian *et al.* [5], it was found that the initial frost dendrites are spherical in shape at about 5–10 μm in diameter. As smooth frost forms, the diameters increase to about 20–50 μm and the ice dendrites begin to mesh together. Biguria and Wenzel observed that initial frost was rough, consisting of ice trees and air spaces. They assumed that parallel heat transfer could be dominant up to a frost density of about 0.02 g cm^{-3}. Then from about 0.02 to 0.05 g cm^{-3} the thermal conductivity was observed to decrease since parallel heat transfer was no longer present when the frost formed a close-knit mesh of dendrites. Then at densities greater than about 0.05 g cm^{-3} the dendrites for thermal conduction began to enclose air pockets. Thus a realistic frost model should somehow allow for changes in conductivity based upon the manner in which a frost structure changes with frost density.

None of the theoretical thermal conductivity expressions listed by Biguria and Wenzel directly provide for such a changing and complicated frost structure. As a matter of caution, it is important to keep in mind that k_e is the air–ice thermal conductivity. The frost thermal conductivity is an expression that will later be derived to include other heat flux terms in equation (1).

2.2. *Argument for negligibility of radiation effective conductivity, k_r*

The radiation effective conductivity can be shown to be negligible for the size of the ice crystals and the temperatures in the frost layer described earlier by the following argument. The radiation effective conductivity as given by Laubitz [6] is,

$$k_r = 4\sigma T^3 \varepsilon (b/\Theta)(1-\Theta^{2/3}+\Theta^{4/3}). \tag{4}$$

An upper limiting value for k_r can be found by setting $T = 273.16$ K, $b = 50$ μm, and $\rho_f = 0.02$ g cm^{-3} for when the ice dendrites begin to mesh together. The result is $k_r < 0.0104$ W m^{-1} °C^{-1}. However, from equations (2) and (3) at the same temperature the thermal conductivities of ice and air are

$$k_i = 2.31 \text{ W m}^{-1} \text{ °C}^{-1} \quad \text{and} \quad k_a = 0.0242 \text{ W m}^{-1} \text{ °C}^{-1},$$

both of which are greater than k_r maximum. Using typical values of $\rho_f = 0.13$ g cm^{-3} and $T = 266$ K [7], gives

$$k_r = 1.43 \times 10^{-3} \text{ W m}^{-1} \text{ °C}^{-1}, k_i = 2.37 \text{ W m}^{-1} \text{ °C}^{-1}$$

and $k_a = 0.0236$ W m^{-1} °C^{-1}. This indicates that a typical radiation effective conductivity will be an order of magnitude less than the thermal conductivity of air. In addition, a typical experimental data of frost thermal conductivity appears to show a noise level around 10^{-3} W m^{-1} °C^{-1} or more. Therefore, the radiation effective conductivity is considered negligible. This was also concluded by White using a different theoretical approach and frost experimental data.

2.3. *Argument for significance of latent heat release—water vapor effective conductivity, k_v*

The concept of the water vapor effective conductivity is obtained by assuming the energy term,

$$L\frac{d\dot{m}_d}{dx},$$

in equation (1) obeys the diffusion equation and meets the condition of water vapor saturation in the frost layer.

The water vapor mass flux is given by the following diffusion equation for the frost by Jones and Parker [8]:

$$\dot{m}_d = \frac{DB}{(1-\chi)\tau_s}\frac{d\rho_v}{dx} \tag{5}$$

where $D = 1.198 \times 10^{-5} T^{1.75} (P_{atm}/P)$ is the ordinary diffusion coefficient fitted to the data ref. [9].

The porosity accounts for the decreased effective cross sectional area for diffusion and the tortuosity, generally taken as 1.1 for frost, accounts for the increased path length the molecules must travel.

The assumption (whose verification is apparent later in Figs. 1 and 2) that the water vapor at the frost surface is saturated implies that the water vapor mass flux can be made to follow the temperature gradient through the gas law

$$P_v = \rho_v R_v T, \tag{6}$$

and the Clapyron equation,

$$P_v = P_v^* \exp\left[\frac{L_s}{R_v T^*} - \frac{L_s}{R_v T}\right]. \tag{7}$$

An expression for

$$\frac{d\rho_v}{dx}$$

is derived by differentiating the gas law with respect to x and the Clapyron equation with respect to temperature. They are substituted into equation (5) to give

$$\dot{m}_d = \frac{DB}{(1-\chi)\tau_s}\left(\frac{P_v}{R_v T^2}\right)\left(\frac{L_s}{R_v T} - 1\right)\frac{dT}{dx}. \tag{8}$$

Since equation (8) directly relates the water vapor mass flux to the temperature gradient, a thermal conductivity due to the water vapor latent heat flux can

be defined by

$$k_v \equiv \frac{\dot{m}_d L_s}{(dT/dx)} = \frac{L_s DB}{(1-\chi)\tau_s}\left(\frac{P_v}{R_v T^2}\right)\left(\frac{L_s}{R_v T} - 1\right). \quad (9)$$

If supersaturation within the frost layer exists, then the Clapyron equation is no longer valid and a new equation for P_v would have to be derived. Fortunately, it was found this is not necessary, as the following derivation from the published experimental data will show.

The situation of supersaturation can be examined by comparing the total mass flux, $\dot{m}_t$, consisting of water vapor, water droplet and ice particles with the water vapor mass flux, $\dot{m}_d$. If one observes that $\dot{m}_t \simeq \dot{m}_d$ for all values of x, then no nucleated drops have formed; this means a supersaturated state is unlikely. If one observes that $\dot{m}_t > \dot{m}_d$ for some values of x, then nucleation or movement of ice particles has occurred and thus supersaturation might be possible. Note that homogenous nucleation and nucleation on nucleating sites in the frost layer cannot be experimentally distinguished. Thus, we cannot state definitely if supersaturation has occurred. If $\dot{m}_d = \dot{m}_t$ at the frost surface, x_s, then we have a good method for predicting the mean frost density growth rate.

If experimental values of the frost density and temperature distribution are known, then the parameters of equation (8) can be derived and the water vapor mass flux can be calculated as a function of the x variable. Observations by several authors [4, 5, 10, 11, 12] indicate that the frost density is nearly spatially invariant in the x direction. This implies that the total water mass flux, $\dot{m}_t$, is given by

$$\frac{d\dot{m}_t}{dx} = \frac{\dot{m}_t}{x} = \frac{\dot{m}_{exp}}{x_s} \quad (10)$$

where $\dot{m}_{exp}$ is the experimentally calculated value of the water mass flux into the frost surface from the surrounding air and x_s is the frost thickness.

Figure 1 shows a plot of $\dot{m}_d$ and $\dot{m}_t$ calculated from an

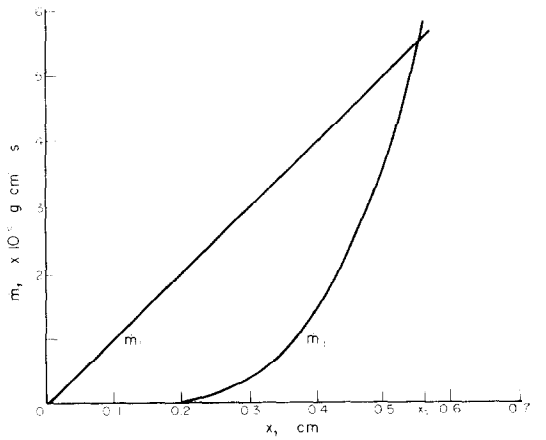

FIG. 1. Water mass flux vs distance in frost layer. (Data of ref. [5].)

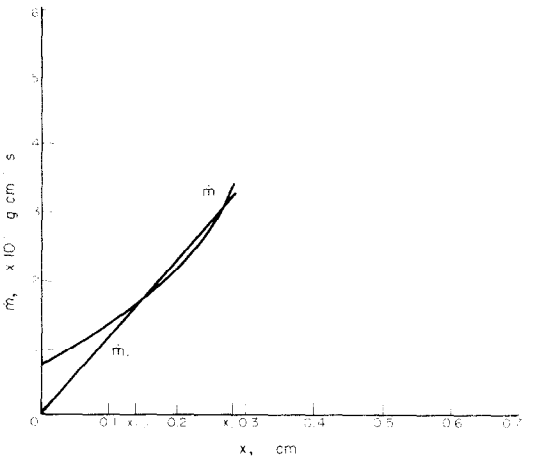

FIG. 2. Water mass flux vs distance in frost layer. (Data of ref. [7].)

experimental data set of Brian *et al.* [5] where the dependent relationship of D and P_v in equation (8) is for the temperature variations from 80 to about 265 K. In comparison to the $\dot{m}_t$ curve, it is probable that some supersaturation has occurred, given the magnitude of the difference between $\dot{m}_t$ and $\dot{m}_d$ although a large contribution can be from the thermal diffusion of ice particles. At distance x_s from the wall we note that $\dot{m}_d$ is equal to $\dot{m}_t$. A data set with a more typical temperature range can be obtained from Yamakawa *et al.* [11]. Here the range of temperature, in one specific case, is from 251 to 269.7 K. Although the experimental temperature distribution within the frost is not available, indications are that for this small temperature range, the temperature profile can be roughly approximated as a linear function of x. Thus, the temperature gradient for equation (8) is given by

$$\frac{dT}{dx} = \frac{T_s - T_w}{x_s} = 6678 \text{ K m}^{-1}$$

as obtained from experimental data in Yamakawa *et al.*; where $x_s = 0.0028$ m. At this frost thickness the frost density is 0.1110 g cm^{-3} and the ambient absolute humidity is 0.0049 as obtained from the data. Substituting these values into equation (8) gives the $\dot{m}_d$ curve shown in Fig. 2. For the top half of the frost layer, the $\dot{m}_d$ curve agrees closely with the $\dot{m}_t$ curve calculated from experimental data, while the lower half of the frost layer, $\dot{m}_d$ is greater than $\dot{m}_t$. These observations mean that at least down to a wall temperature of 251 K we can confidently say the frost layer is in a saturated state. In addition, at the distance x_s, we find that $\dot{m}_d = \dot{m}_t$. The conclusion is that the water vapor thermal conductivity expression, equation (9), is at least valid for most, and should be valid for all, frost formation situations and a method for calculating the water mass flux entering the frost surface has been obtained.

Now k_v can be compared directly with k_a and k_i for an order of magnitude analysis. From ref. [7], with the same data used in evaluating the radiation effective

conductivity, we obtain at the frost surface, using equation (9), $k_v = 0.0111$ W m^{-1} °C^{-1}.

Since $k_a = 0.0236$ W m^{-1} °C^{-1}, the water vapor thermal conductivity cannot be ignored at very low frost density. At higher frost density, k_v actually decreases and becomes minimal due to the porosity term in equation (9). At close to ice density the term $k_i = 2.37$ W m^{-1} °C^{-1} indicates the dominating influence of k_e. So far, the order of magnitude calculations show that particular attention must be devoted to developing the air–ice thermal conductivity which would include a complicated frost structure modeling and perhaps also the water vapor thermal conductivity at low frost density.

2.4. *Argument for negligibility of ventilation enthalpy rate term,* $G_a C_p \dfrac{\partial T}{\partial x}$

The effective air mass flux, G_a, is quite difficult to determine because it is strongly dependent on the frost structure. Since the wall is impermeable (i.e. no suction or blowing underneath the frost layer) the only forced air sources are convective turbulent eddies and the total water mass flux. For frost density less than 0.02 g cm^{-3}, Biguria and Wenzel considered the convective turbulent eddies to dominate the heat transfer in the frost layer and then diminish as the frost density approaches 0.048 g cm^{-3} due to the close-knit mesh of dendrites. Biguria and Wenzel used a radiometer to measure the frost surface temperature in deriving the frost thermal conductivity. However, for an optically thin frost layer the frost surface temperature will be read much too low, using a radiometer, thus resulting in a thermal conductivity too high. Thus the correlations by Biguria and Wenzel for the eddy contribution to the mean frost thermal conductivity are largely fictitious. Furthermore, from theoretical considerations the eddy contribution to the mean frost thermal conductivity should be negligibly small. This eddy contribution was related to the free-stream velocity by Biguria and Wenzel when it should instead be a function of the nondimensional variable $x^+ = xu_v/\nu$. More specifically, in the turbulent sublayer the eddy conductivity or the eddy diffusity is proportional to $(x^+)^3$ and in the turbulent core it is proportional to x^+ for either smooth or rough wall. Thus, the contribution of convective turbulent eddies is small near the wall. Besides that, the model of the total water flux $\dot{m}_t$, at the frost surface, as discussed in the previous section, is directly related to the diffusion flux, which requires the air in the frost layer to be stagnant. Therefore, in the modeling of frost growth the initial frost density will be high enough so that there are no eddies in the frost layer. In summary, since turbulent eddies are considered negligible, the only mass flux within the frost layer is the total water flux, $\dot{m}_t$, which is set equal to G_a. The specific heat of ice C_{p_i} is also set to C_p as a conservative estimate.

Using the same data of Brian *et al.* which was used to evaluate k_v and k_r, an upper estimate is made of the forced-air enthalpy rate term in equation (1) for comparison with the latent heat term. Since $\dot{m}_{d_s} = \dot{m}_{t_s}$ and the measured temperature gradient is a maximum at the surface, the upper estimate is calculated as

$$\dot{m}_{d_s} C_{p_i} \left.\frac{dT}{dx}\right|_s = 1620 \text{ W m}^{-3}.$$

This can be compared to a lower estimate of the latent heat contribution calculated at the frost surface by

$$L_s \frac{d\dot{m}_{d_s}}{dx} \geqslant L_s \frac{d\dot{m}_{t_s}}{dx} = L_s \frac{\dot{m}_{t_s}}{x_s} \simeq L_s \frac{\dot{m}_{d_s}}{x_s} = 29\,100 \text{ W m}^{-3}.$$

A comparable result is also obtained for calculations within the frost layer. Therefore, the heat transfer rate by the effective forced-air enthalpy term is much lower than the latent heat release within the frost layer. In a different approach and experiment, White has also found the effective forced-air enthalpy term to be negligible. Another consideration is the snow ventilation correlation by Yen [13] for a mass flux of $\dot{m}_{t_s} = 0.06$ g m^{-2} s^{-1} as was used in the above equation. The thermal conductivity contribution of this mass flux turns out to be 0.0015 W m^{-1} °C^{-1}. Again, this is quite small compared to $k_a = 0.0236$ W m^{-1} °C^{-1} and $k_i = 2.37$ W m^{-1} °C^{-1} used in comparison for k_v and k_r.

Since the experimental data are not accurate to three or four significant digits as would be required both by the effective forced-air enthalpy rate and the radiation heat rate, the terms for the conductive heat rate and the latent heat release rate are the only terms retained in equation (1). The result is

$$\frac{d}{dx}\left[k_e \frac{dT}{dx}\right] = -L\frac{d\dot{m}_d}{dx} = -\frac{d}{dx}\left[k_v \frac{dT}{dx}\right]. \quad (12)$$

Integration of the above equation gives

$$K\frac{dT}{dx} = q_0 \quad (13)$$

with

$$K = k_e + k_v$$

where q_0 is a constant heat flux at the wall and K is the thermal conductivity of frost. With the simplified equations above, other approaches obtained from the literature for calculating the frost thermal conductivity can be evaluated.

3. PUBLISHED APPROACHES FOR CALCULATING K

If the heat flux and the temperature gradient are measured as was done in the frost experiments of Brian *et al.* [7] and Shah [10], a frost thermal conductivity can be calculated easily from the above equations. It is important that the experimental heat flux should be measured at the wall, as previously [7, 10], rather than

at the frost surface. The reason is that, due to the latent heat contribution, the heat flux becomes lower at the frost surface than at the wall.

An empirical expression for the thermal conductivity of frost, based on the experimental data of Brian *et al.* [7] and Shah and Brazinsky [14], was developed by Brian *et al.* [5]. The expression for thermal conductivity is a linear function of frost density and a power function of temperature. If Brian *et al.*'s empirical frost thermal conductivities as a function of temperature [5] are calculated for high frost densities then they do not approach the thermal conductivity of ice k_i as should be required. Similarly, if the same is done on the basis of air density, the resulting curves show some disagreement with the actual thermal conductivity of air, k_a. Furthermore, the validity of this approach is experimentally restricted to frost densities less than 0.13 g cm^{-3}, low wall temperatures and ambient humidities, as indicated in Table 1.

In another approach, White [1] formulated the effective thermal conductivity k_e as a linear function of frost density and temperature. Also, he provided an estimation for water vapor thermal conductivity k_v. Then White combined the terms k_e and k_v and arrived at an expression for K that fits the Shah data. This approach, although more theoretical, is subject to the same limitation as the previous approach.

Since the water vapor diffusion occurs only in the air portion of the frost, Biguria and Wenzel [4] suggest that if the effective air thermal conductivity instead of the true air thermal conductivity is used, one can expect better results. The effective air thermal conductivity can be obtained from the relation

$$k_{\text{eff air}} = k_a + \frac{DP_t}{P_t - P_v}\left(\frac{L_s P_v}{R_v T^2}\right)\left(\frac{L_s}{R_v T} - 1\right) = k_a + \frac{\tau_s k_v}{B} \quad (14)$$

where P_t is the ambient pressure, which is based on equation (21) of Biguria and Wenzel [4] and equation (9). It may be noted that for obtaining the air effective conductivity, the tortuosity and the porosity expressions in the vapor effective conductivity are neglected since they are not applicable to the air portion of the frost. According to Biguria and Wenzel, one can obtain a better expression for k_e by using $k_{\text{eff air}}$ instead of k_a in the theoretical models used in their work. For frost densities greater than 0.05 g cm^{-3}, Biguria and Wenzel claimed that a good fit to their experimental data was obtained by using this approach. The experimental thermal conductivity of frost was obtained, however, by measuring the heat flux at the wall, the thickness of the frost and the wall and frost surface temperatures. In order to apply the theoretical thermal conductivity equations to the data, Biguria and Wenzel implicitly assumed the frost layer has uniform temperature, structural and density distributions. These assumptions require a high wall temperature at approximately 250 K, the frost to be formed in a specified structure, and the ambient absolute humidity to be in a specified range near saturation. In contrast, the data of Brian *et al.* [5] and Shah [10] typically have the wall temperature at 80 K, with more spherical ice formations than ice trees and an ambient absolute humidity at a fraction of the saturation level. Thus it is expected the approach by Biguria and Wenzel will not fit satisfactorily to the data of Brian *et al.* [5] and Shah [10]. This actually turned out to be the case. The basic disadvantage of the Biguria and Wenzel approach is the requirement of a uniform temperature and uniform structural distribution of the frost.

Assuming that the frost density is spatially invariant so that the amount of water vapor forming frost is the same at all locations in the frost layer allows the calculation of the change in the vapor mass flux with distance as

$$\frac{d\dot{m}_d}{dx} = \frac{\dot{m}_{d_s}}{x_s} \quad (15)$$

where $\dot{m}_{d_s}$ is the water flux driven by the temperature gradient at the frost surface. Jones and Parker [8] have

Table 1. Summary of approaches to calculating frost thermal conductivity

Approach	Range of application	Modeling technique	Modeling of the frost structure
Brian *et al.* [5]	$0.05 < \rho_f \leq 0.13$ g cm^{-3}	Empirical	None
White [1]	$0.05 < \rho_f \leq 0.13$ g cm^{-3}	Semi-empirical	Vapor diffusion in frost layer is postulated
Biguria and Wenzel [4]	0.05 g cm$^{-3} < \rho_f < \rho_{ice}$	Theoretical	Simple frost structures and vapor diffusion is postulated
Jones and Parker [8]	$0.05 < \rho_f \leq 0.13$ g cm^{-3}	Semi-empirical	Vapor diffusion in frost layer is postulated
Putman and Zuckerman [15]	$0.1 < \rho_f < 0.48$	Mostly theoretical Partly empirical	Ice spheres connected by cylinder ice columns
Present approach	$\rho_a < \rho_f < \rho_{ice}$ 80 K $< T_w <$ 273 K	Mostly theoretical Partly empirical	Complicated frost structure is postulated for vapor diffusion, geometrical shapes of ice dendrites, and for frost aging

used this relationship to model the heat transfer mechanism in the frost layer. This also allows deriving a model for the frost thermal conductivity. Substituting the above expression into equation (12) and integrating, we get

$$k_e \frac{dT}{dx} = \frac{-L_s \dot{m}_{d_e} x}{x_s} + q_0. \quad (16)$$

It may be noted that k_e does not contain the expression for $k_{eff\,air}$. Because Jones and Parker used the Brian *et al*'s [5] empirical frost thermal conductivity, this approach is limited to frost density less than 0.13 g cm^{-3}. If a linear vapor mass flux with distance which releases the latent heat is assumed, then, because of what has been shown in Figs. 2 and 3, a supersaturated state would have to exist in Brian *et al*'s data [5] and a subsaturated state would have to exist in Yamakawa's data within the frost layer. This dual state is physically unlikely.

In the last approach examined, Pitman and Zuckerman [15] claimed to have measured and correlated the effective thermal conductivity of snow at 185, 246, and 268 K. Their "snow" was, "composed of vapor-grown ice crystals . . . on the walls of a freezer supplemented by dry ice. A bath of distilled water at a controlled temperature was used as the vapor source." This statement proves that they were forming frost rather than snow. "The conductivity is measured by a guarded cut-bar apparatus with Plexiglas as the bar material." (ref. [15], p. 2698) This apparatus allows one to keep a fairly constant temperature in the uniform frost layer. Thus the effective thermal conductivity was measured as a function of the frost density and temperature over the range of frost density from 0.1 to 0.6 g cm^{-3} and of frost temperature from 185 up to 268 K. For correlating with the data they modified the Woodside thermal conductivity equation [4] for a cubic lattice of uniform solid spherical particles in a gas to include the connecting ice cylinder columns with the radius of the ice cylinder as an empirical parameter. The theoretical limit of this model is the maximum frost density at 0.48 g cm^{-3}. As a last comment, they did not include a vapor thermal conductivity, k_v, into their expression for K in equation (13).

When some previously described experimental data could not be fitted to the theoretical approach suggested by Biguria and Wenzel, an attempt was made to see if the experimental values of frost thermal conductivity given by Brian *et al.* could lie between the curves represented respectively by the thermal conductivity equations for either spherical air pores or spherical ice particles. The encouraging results in Fig. 3 showed that the frost thermal conductivity is a linear function of porosity or frost density for porosities greater than 0.85. This gave a motivation to propose a new model, based on Biguria and Wenzel's theoretical approach, but which includes frost structure parameters which could be empirically derived to fit Brian *et al.*'s data, Pitman and Zuckerman's [15] data, as well as other data.

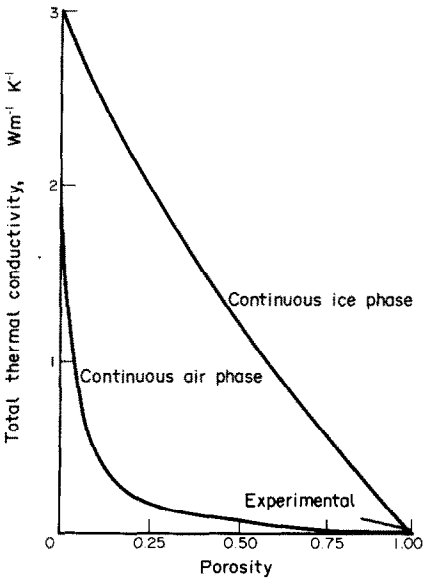

FIG. 3. Thermal conductivity vs frost porosity at 211 K.

4. THE PRESENT APPROACH FOR CALCULATING K

The proposed model makes the following assumptions about the frost structure, as shown in Fig. 4. At low frost density or at high porosity, two types of frost structure predominate. One is the ice cylinders created by the diffusion of water onto the ice, which result in a parallel conductive heat transfer. The other portion is the ice spheres created by nucleation of water vapor or

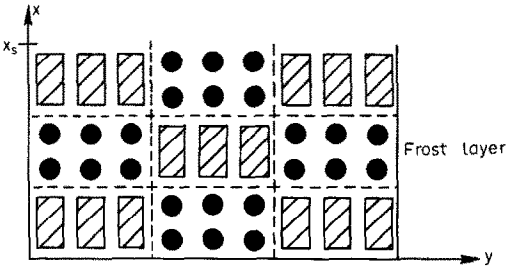

FIG. 4(a). Frost structure model of the present work. Random mixture of ice cylinders and ice spheres at high porosities or low frost densities.

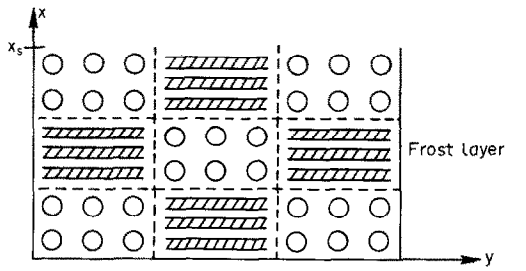

FIG. 4(b). Frost structure model of the present work. Random mixture of ice planes and air bubbles at low porosities or high frost densities.

water droplets, resulting in a much lower conductive heat transfer. The total structure of the frost is then the random mixture of ice cylinders and ice spheres [Fig. 4(a)]. At high frost density or low porosities, completely different dual structures begin to take shape. In contrast to the low density case, spherical air voids are formed in place of ice cylinders [Figure 4(b)]. This results in enhanced thermal conduction. Also, in place of the ice spheres, stratified layers are formed. The total frost structure is then a random mixture of air bubbles and ice layers.

With such a model of the frost structure, the equations for air–ice thermal conductivity are combined as follows. First the thermal conductivity of air bubbles and ice cylinders are close to each other at all porosities. Similarly, the thermal conductivities of ice planes and ice spheres, though considerably less than of ice cylinders and ice bubbles, are close together at all porosities. Thus, an upper limit conductivity expression was derived for the air bubbles and ice cylinder structures that at its low porosity limiting value ($B = 0$) takes on the thermal conductivity of air bubbles and at its high porosity limiting value takes on the thermal conductivity of ice cylinders. Similarly a lower limit expression combining the thermal conductivities of ice spheres and ice planes with appropriate limiting values has been derived. Finally, an expression for frost thermal conductivity at all porosities is derived by combining the upper and lower limit expressions. The upper limit conductivity expression for air bubbles and ice cylinders is

$$k_u = (1-B)k_b + Bk_c \text{ (upper limit)} \tag{17}$$

where the thermal conductivity of air bubbles is given by

$$k_b = k_i\left[1-2B\left(\frac{1-a}{2+a}\right)\right]\Big/\left[1+B\left(\frac{1-a}{2+a}\right)\right], \tag{18}$$

$$a = k_{\text{eff air}}/k_i \quad [4]$$

and ice cylinders by

$$k_c = (1-B)k_i + Bk_{\text{eff air}} \quad [4]. \tag{19}$$

Likewise, the lower limit of thermal conductivity is formed by an interpolation between thermal conductivities for ice spheres and ice planes,

$$k_l = (1-B)k_p + Bk_s \text{ (lower limit)} \tag{20}$$

where the thermal conductivity of ice spheres is given by

$$k_s = k_i[3+2B(a-1)]\Big/\left[3-B\left(\frac{a-1}{a}\right)\right] \quad [4] \tag{21}$$

and ice planes by

$$k_p = \frac{k_i k_{\text{eff air}}}{(1-B)k_{\text{eff air}} + k_i B} \quad [4]. \tag{22}$$

To combine the contribution of the structures that represent the upper and the lower limits of the thermal conductivity to the frost thermal conductivity, the random mixture model of Brialsford and Major from Biguria and Wenzel [4] is utilized. This gives the thermal conductivity of frost as

$$K = 1/4((3B_c-1)k_l+(3\Theta_c-1)k_u + \{[(3B_c-1)k_l+(3\Theta_c-1)k_u]^2+8k_lk_u\}^{1/2}) \tag{23}$$

where B_c is the proportion of the frost volume representing ice spheres and ice planes. It is defined by a polynomial function of the porosity B as

$$B_c = \sum_{i=0}^{n} a_i B^i. \tag{24}$$

The a_i's can be evaluated as constants or as functions of temperature. The other portion of the frost volume representing ice cylinders and air bubbles is given by

$$\Theta_c = 1 - B_c. \tag{25}$$

4.1. *Comparison of local frost thermal conductivity to data*

It is plausible to assume the frost takes on a complete air bubble structure when the frost porosity approaches zero or the frost density approaches that of ice. This assumption when translated to the boundary condition for equation (24) gave $B_c = 0$ for $B = 0$, and thereby a_0 was found to be zero. To make any further progress with the coefficients a_i the experimental data of Brian *et al.* [5] as shown in Fig. 5 and of Pitman and Zuckerman [15] as shown in Fig. 6 was utilized. Since the data of Pitman and Zuckerman show the frost density range of 0.1–0.6 g cm^{-3}, it was fitted first for the various values of n. The best fits occurred for $n = 2$ and 4. Higher values of n were not attempted because the coefficients a_i are functions of temperature. The curve fittings to Brian *et al.* data [5] for $n = 2$ and 4 worked well also. But when the coefficients a_i were compared between the two data sets it was found the coefficients a_i provided the most

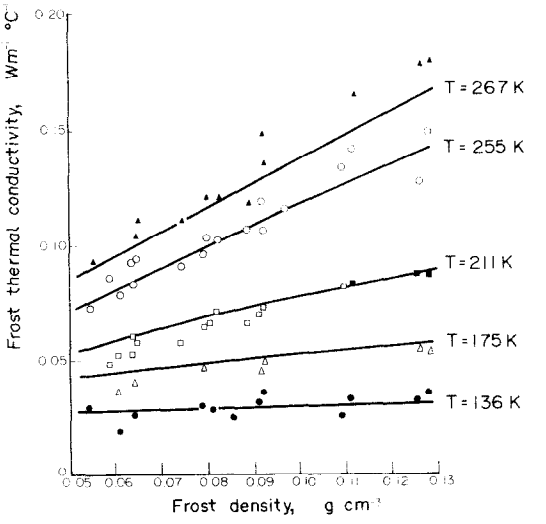

FIG. 5. Comparison of the present frost thermal conductivity model with the experimental data of Brian *et al.* [5] as a function of frost density and temperature.

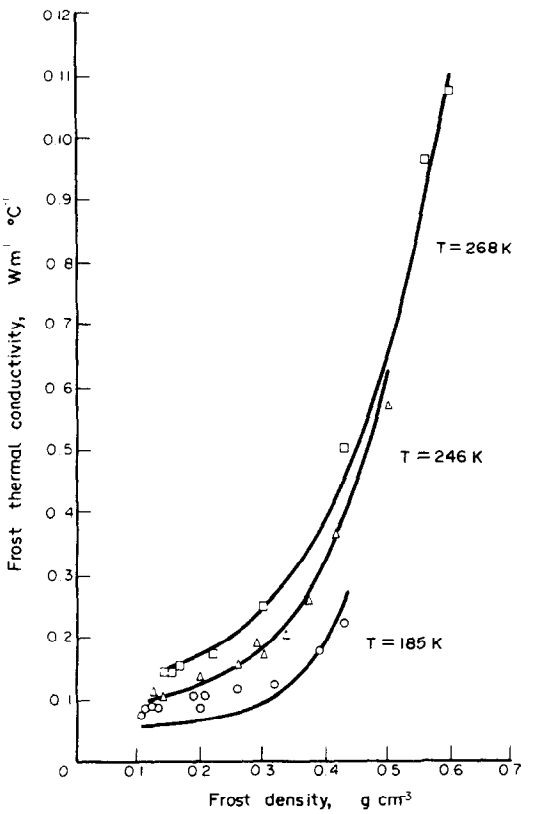

FIG. 6. Comparison of the present frost thermal conductivity model with the experimental data of Pitman and Zuckerman [15] as a function of frost density and temperature.

consistency for $n = 4$. The difficult problem of finding the temperature dependent behavior of the coefficients a_i was simplified by rearranging the polynomial equation for B_c to represent the local extremes of the fourth degree polynomial. The fit to Pitman and Zuckerman data [15] in Fig. 6 finally resulted in the equation

$$B_c = 13.6(B_2-B_1)(B-B_1)^2 \times \left[1-\frac{2}{3}\left(\frac{B-B_1}{B_3-B_1}+\frac{B-B_1}{B_2-B_1}\right)+\frac{(B-B_1)^2}{2(B_3-B_1)(B_2-B_1)}\right] \quad \text{for} \quad B > B_1$$

$$B_c = 0 \quad \text{for} \quad B \leqslant B_1 \tag{26}$$

where

$$B_1 = 0.1726(T/273.16),$$
$$B_2 = 0.751, \tag{27}$$
$$B_3 = B_2+0.3.$$

Thus the effective coefficient, B_1, was the only coefficient that was a simple function of the frost layer temperature, T. The value of B_1 can be interpreted as the frost porosity below which the frost layer can simply be described as air bubbles. The above formulation, was modified slightly to fit Brian *et al.*'s data [5] as shown in Fig. 5 by redefining B_3 as

$$B_3 = B_2+0.3 \sin\left[\left(\frac{\pi}{2}\right)\frac{1-(T/273.16)^2}{1-(T_w/273.16)^2}\right]. \tag{28}$$

This can be interpreted as the effect the water vapor flux has on altering the structure of the frost. Referring to Fig. 1, we see that most of the vapor flux is in the upper half of the frost layer, thus predisposing the frost structure toward ice cylinders. In the lower half of the frost layer where the vapor flux is minimal more spherical nucleated particles are expected. As a result, B_3 goes to $B_2+0.3$ in the limit as T approaches the wall temperature, T_w. The function B_c as formulated up to this point provides a good description of frost aging as the frost density increases.

4.2. *Comparison of average frost thermal conductivity to data*

In order to compare the frost thermal conductivity, as predicted from the proposed model, to other experimental data, which lacked sufficient measurement detail, an average frost thermal conductivity is needed. The average frost thermal conductivity, denoted by $\bar{K}$, is defined by Brian *et al.* and here as,

$$\bar{K} = \int_{T_w}^{T_s} K \, dT/(T_s-T_w). \tag{29}$$

To calculate such an average frost thermal conductivity, a frost formation model must also be used concurrently to calculate the frost surface temperature T_s, the frost density, and the frost thickness as a function of time. The present frost formation model is an outgrowth of that described in ref. [16]. The only data found on the average frost thermal conductivity in which the frost formation model could be used concurrently were that of Brian *et al.* [5], Yamakawa *et al.* [11], Nakamura [12], and Yonko and Sepsy [17] as shown in Fig. 7.

The calculation of average frost thermal conductivity by equation (29) with the concurrent frost formation model has resulted in the curve a, which fits Brian *et al.*'s [5] data very well below 0.13 g cm^{-3}. The frost formation model was then used to continue the computation of the frost growth above frost density of 0.13 g cm^{-3} until the ice density was reached. This resulted in the curve a in Fig. 7 plotted up to a frost density of 0.6 g cm^{-3}. One will note the similarity between curve a in Fig. 7 with the 185 K curve in Fig. 6, indicating that curve a is reasonable. If one also compares curve a in Fig. 7 to Brian *et al.* [5] data in Fig. 5 one sees that the low temperature region of the frost layer dominates the average frost thermal conductivity. With this confidence in the average frost thermal conductivity the data by Yamakawa *et al.* and Nakamura, and Yonko and Sepsy were then examined.

If one looks closely at the experimental techniques and analytical procedures of Yamakawa *et al.* for

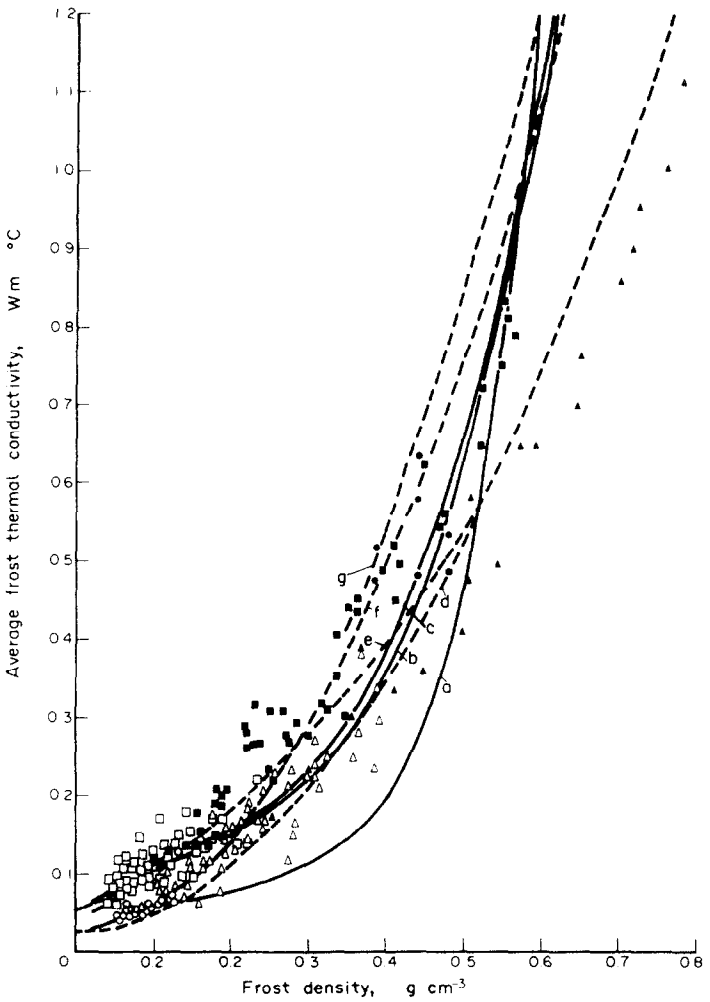

FIG. 7. Comparison of the present average frost thermal conductivity model with various experimental data and correlations as a function of frost density. ○, Brian *et al.* [5]; ●, Coles [18]; ■, Yonko and Sepsy [16]; △, Yamakawa *et al.* [11]; □, Nakamura [12]; ▲, Feniger [19]; a, model curve to ○ data; b, model curve to △ data; c, model curve to □ and ■ data; d, Lotz [21]; e, Kamei [22]; f, Devaux [23]; g, Kondrat'eva [24].

obtaining the data shown by open triangles in Fig. 7, one concludes the scatter was caused mostly by inaccurate frost densities, especially at low values. This is due to their method of scraping and weighing the frost at a given time, rather than the more accurate method of using the tare weight of the cooled plate as was done by Nakamura. But on the other hand, if one looks closely [12] at experimental techniques and analytical procedures for obtaining the data shown by open squares in Fig. 7, one concludes the scatter was caused mostly by inaccuracies in the frost thermal conductivity. This is due to their method of obtaining heat flux through the frost layer by combining sensible, latent, and radiant heat flux at the frost surface rather than measuring the heat flux underneath the frost layer as was done by Yamakawa *et al.* Yonko and Sepsy did measure heat flux underneath the frost layer and used the tare weight method of obtaining the frost density. But their method of measuring the frost surface temperature by turning off the air blower and lowering a thermocouple to the frost surface would give an average frost thermal conductivity biased too high as shown by the closed squares on Fig. 7. Especially at the lower frost density, the frost layer is more easily disturbed and subjected to transient conditions. Thus, the Yonko and Sepsy data can be used beyond the frost density limits at 0.4 g cm^{-3} of Yamakawa *et al.*'s data. In turn the Yamakawa *et al.* data can be used beyond the frost density limits at about 0.2 g cm^{-3} of Nakamura's data.

As was demonstrated by curve a in Fig. 7, the formulation for B_c covers the full range of frost density. But if the structure parameter B_c given by equation (26) is used in calculating $\bar{K}$ concurrently with a frost formation model, the curves predicted for $\bar{K}$ become too high as compared to data of Yamakawa *et al.* and Nakamura. This implies that B_c given by equation (26) is too low for these data.

A problem that has not yet been addressed is how the saturation ratio, $R = w_a/w_w$, where w_a is the free stream

humidity and w_w the humidity at the wall temperature, affects the structure of the initial frost layer. Biguria and Wenzel in their study of very low frost density observed that the frost grew according to a critical cluster mechanism. We propose this mechanism is the result of the dynamics of nucleated water droplets. According to Rosner and Epstein [18] when the saturation ratio, R, gets high enough a boundary layer fogging appears. Then when R is very large the number density of fog particles will reach the number density of nucleation sites as a limit. If there are nucleation sites on the plate itself, nucleated drops will form there even for low values of the saturation ratio, R. Thus when R is low enough the initial frost layer will consist mostly of somewhat spherical frozen droplets. But when R is high enough for the boundary layer fogging to also appear, the probability of droplet coalescence on a partially frozen droplet on the wall increases. This results in a distortion of the initial frost element shapes from the spherical. The data of both Brian *et al.* and Pitman and Zuckerman are for very high values of R, thus making the correlation of B_c with R for these two data sets impossible. But we note that for a very high value of R the number density of fog particles reaches a limit, which translates into a maximum possible distortion of the initial frost element shapes from a spherical shape. Since the function B_c represented by equation (26) represents that limit, B_c can be postulated as a simple inverse relationship to R. After trying various functional forms for the correction to B_c due to R, the fit to Nakamura's data in the 0.05–0.23 g cm^{-3} region, to Yamakawa *et al.*'s data in the 0.2–0.4 g cm^{-3} region, and to Yonko and Sepsy's data in the 0.4–0.6 g cm^{-3} region resulted in the correction equation to B_c as,

$$R_c = 1 + \frac{0.5264}{R}, \tag{30}$$

so that as R approaches one, B_c is corrected by the maximum amount of 1.5264. When R is less than one, no nucleated water droplets exist either in the air or on the wall, and thus there is no frost formation. R_c has been validated only for R as low as 2. With the correction to B_c given by R_c, the curve b in Fig. 7 corresponds to the open triangle data. The curve c in Fig. 7 corresponds to both the open squares at frost density less than 0.23 g cm^{-3} and the closed squares at frost density greater than 0.4 g cm^{-3}. The closed circle data of Coles [19] and the closed triangle data of Feniger [20] provide further comparisons at high frost density. But for these two data sets the average temperature of the frost layer and their experimental techniques are not known to us. Cole's data has a lot of scatter, but they lie within the limits of Yonko and Sepsy's data.

To further establish the validity of curves b and c in Fig. 7, comparisons are made with published correlations of average frost thermal conductivity versus frost density at average frost temperature close to freezing. The correlation of Lotz [21] is the curve d in Fig. 7. Lotz's own data validated his correlation for a frost density up to 0.4 g cm^{-3}. He extrapolated the correlated curve beyond 0.4 g cm^{-3} simply to compare with Feniger's data [20]. Another correlation cited quite often in the literature is that of Kamei [22] as shown by the curve e in Fig. 7. Even Kamei's correlation shows that Yonko and Sepsy's data is biased too high. The curve c seems to straddle around Kamei's correlation represented by curve e, up to a frost density of 0.5 g cm^{-3}. But curve c remains above Lotz's correlation represented by curve d. Finally, Devaux's [23] and Kondrateva's [24] correlation for snow are shown by curves f and g respectively in Fig. 7. Yen's [13] correlation for no ventilation in snow lies in between curves f and g. We note the snow correlations follow a different pattern than the frost for the average thermal conductivity at low frost or snow density. This means the compression of snow results in a different structural pattern than a frost growing without mechanical restraints. Yet, intuitively, at high densities the snow should take on an air bubble structure similar to frost. Thus at the frost density of 0.6 g cm^{-3} the curves b and c in Fig. 7 seem to be converging with curves f and g. When Figs. 5, 6 and 7 are taken together one sees that a complicated, but an excellent model of the frost thermal conductivity has been constructed.

5. CONCLUSIONS

(1) It was found that of the several models of the frost thermal conductivity found in the literature, none was suitable for a general frost formation model as demonstrated by an order of magnitude analysis and by consideration of theoretical limitations.

(2) Since it was desired to approach the proper thermal conductivities in the limit of ice or air density, a theoretical model of a random mixture of ice cylinders and ice spheres at low frost densities or of air bubbles and ice planes at high frost densities was postulated.

(3) The so called water vapor conductivity was included with the air thermal conductivity as per Biguria and Wenzel's [4] suggestion. But the eddy conductivity was not included for various reasons. The radiation and the forced-air-flow conductivities were shown to be negligible by an order of magnitude analysis.

(4) In order to fit the data of Brian *et al.* [5] and Pitman and Zuckerman [15] using the theoretical model of frost thermal conductivity thus developed, the structural parameter B_c represented by the fraction of the frost layer in the form of ice spheres and ice planes was fitted mainly as a function of the frost porosity and partly as a function of the local frost temperature and of the wall temperature. The result is given by equations (26)–(28) and shown in Figs. 5 and 6.

(5) An average frost thermal conductivity was computed by equation (29) concurrently with a frost formation model to compare with the large data set published in the literature. The structural parameter, B_c, was modified slightly as in equation (30) to account for the effect of the initial saturation ratio R on the frost

structure, and thus also the frost thermal conductivity. The result is shown in Fig. 7 and comparisons with correlations found in the literature of the average frost thermal conductivity has shown the reasonableness of the present frost thermal conductivity model. It is expected that if any new comprehensive data are published, then the coefficients in the expression for B_c should be re-examined.

Acknowledgements—This research was sponsored by the National Aeronautics and Space Administration, Marshall Space Flight Center, Space Sciences Laboratory, Atmospheric Sciences Division, under Contract NAS8-33369. The author is indebted to Mr A. Richard Tobiason of the Office of Aeronautics and Space Technology, NASA Headquarters, for support of this research and to Mr Dennis Camp of Marshall Space Flight Center for his assistance as Technical Monitor.

REFERENCES

1. J. White, Heat and mass transfer in thick frost layers, Ph.D. dissertation, University of Kentucky, Mechanical Engineering Department (1973).
2. W. M. Rohsenow and J. P. Hartnett, *Handbook of Heat Transfer*. McGraw-Hill, New York (1973).
3. D. S. Dillard and K. D. Timmerhaus, Low temperature thermal conductivity of selected dielectric crystalline solids, in *Thermal Conductivity, Proceedings of the 8th Conference* (edited by C. T. Ho and R. E. Taylor), pp. 949–967. Plenum Press, New York (1969).
4. G. Biguria and L. A. Wenzel, Measurement and correlation of water frost thermal conductivity and density, *I&EC Fundamentals* **9**, 129–138 (1970).
5. P. L. T. Brian, R. C. Reid and I. Brazinsky, Cryogenic frost properties, *Cryogenic Technol.* **5**, 205–212 (1969).
6. M. M. Laubitz, Thermal conductivity of powders, *Can. J. Phys.* **37**, 798–808 (1959).
7. P. L. T. Brian, R. C. Reid and Y. T. Shah, Frost deposition on cold surfaces, *I&EC Fundamentals* **9**, 375–380 (1970).
8. B. W. Jones and J. D. Parker, Frost formation with varying environmental parameters, *Trans. Am. Soc. Mech. Engrs* Series C, *J. Heat Transfer* **97**, 255–259 (1975).
9. New York American Society of Heating and Air Conditioning Engineering, *Heating, Ventilating, Air Conditioning Guide*, Vol. 37, pp. 22–25 (1959).
10. Y. T. Shah, Sc.D. Thesis, M.I.T. (1968).
11. N. Yamakawa, N. Takahashi and S. Ohtani, Forced convection heat and mass transfer under frost conditions. *Heat Transfer-Japan. Res.* **1**, 1–9 (1972).
12. H. Nakamura, Free convective heat transfer from humid air to a vertical plate under frosting conditions, *Bull. JSME* **17**, 487–494 (1974).
13. Y.-C. Yen, Effective thermal conductivity and water vapor diffusivity of naturally compacted snow, *J. Geophys. Res.* **70**, 1821–1825 (1965).
14. I. Brazinsky, Sc.D. Thesis, M.I.T. (1967).
15. D. Pitman and B. Zuckerman, Effective thermal conductivity of snow at −88°, −27°, and −5°C, *J. Appl. Phys.* **38**, 2698–2699 (1967).
16. M. A. Dietenberger, A frost formation model and its validation under various experimental conditions, NASA Contractor Report 3595, August (1982).
17. J. D. Yonko and C. F. Sepsy, An investigation of the thermal conductivity of frost while forming on a flat horizontal plate, Paper No. 2043, presented at ASHRAE 74th Annual Meeting, Minneapolis, MN, 26–28 June (1967).
18. D. E. Rosner and M. Epstein, Fog formation conditions near cool surfaces, *J. Colloid Interface Sci.* **28**, 60–65 (1968).
19. W. D. Coles, Experimental determination of thermal conductivity of low density ice, Nat. Adv. Comm. for Aeronautics, Techn. Note. 3143 (1954).
20. K. Feniger, Contribution à l'étude de la transmission de froid avec condensation exterieure, These, Paris (1948).
21. H. Lotz, Heat and mass transfer processes in air radiators, with laminated fins covered with frost in relation to their operating behaviour (in German) pp. 208–217, Kaltetechnik-Klimatisierung, 23. Jahrgang, Heft 7 (1971).
22. S. Kamei, T. Mizushima, S. Kifune and T. Koto, Research on frost formation in a low temperature dehumidifier, *Chem. Engng, Japan* **14**, 53 (1950).
23. J. Devaux, Radiothermic economy of fields of snow and glaciers, *Science Abstr. Series A.* **36**, 980–981 (1933); abstracted from *Ann. d. Phys.* **20**, 5–67 (1933).
24. A. S. Kondrateva, Thermal conductivity of snow cover and physical process caused by the temperature gradient, S.I.P.R.E. Translation No. 22 (1954).

FORMULE GENERALE DE LA CONDUCTIVITE THERMIQUE DE L'EAU GELEE

Résumé—L'étude de la formation du gel a gagné un renouveau d'intérêt. Fondamental pour le développement d'un modèle est l'établissement de la conductivité thermique du gel, ce qui est le sujet de cette étude. La conductivite thermique de la couche de gel joue un rôle important dans sa structure et dans la vitesse de formation. Des articles publiés concernent le problème du calcul numérique de la conductivité. On examine ici les différentes approches en analysant les hypothèses qui sont faites. On discute de tous les mécanismes de transfert possibles dans la couche de gel, pour déterminer quels mécanismes sont significatifs et quels autres peuvent être négligés. A partir de cela, les différentes approches peuvent être évaluées et les résultats comparés avec les données expérimentales. Du plus les domaines de conditions environnementales valables pour les approches sont déterminés. On montre qu'aucune de ces approches n'est suffisant pour un modèle général du gel. Enfin on développe une nouvelle méthode, plus compréhensive, de calcul de la conductivité thermique basé à la fois sur la théorie et les données expérimentales.

EINE ALLGEMEINE BEZIEHUNG FÜR DIE WÄRMELEITFÄHIGKEIT VON REIF

Zusammenfassung—In den vergangenen Jahren erlangten Untersuchungen zur Reifbildung neues Interesse. Entscheidend für die Entwicklung des Reifbildungsmodells war die Herleitung der Wärmeleitfähigkeit der Reifschicht, die der Gegenstand dieser Arbeit ist. Die Wärmeleitfähigkeit einer Reifschicht spielt eine wichtige Rolle für deren Struktur und Bildungsgeschwindigkeit. Eine Anzahl von Veröffentlichungen behandelte die Problematik der Berechnung der Wärmeleitfähigkeit des Reifs. In dieser Arbeit wurden die verschiedenen Ansätze dieser Veröffentlichungen auf die ihnen zugrundegelegten Annahmen hin untersucht. Ein Gesamtverständnis dieser Annahmen beginnt mit einer Gegenüberstellung aller möglichen Wärmetransportprozesse innerhalb der Reifschicht, um die signifikanten Vorgänge von denen unterscheiden zu können, die mit Sicherheit vernachlässigbar sind. Von diesem Ausgangspunkt können die verschiedenen Ansätze der Veröffentlichungen ausgewertet und deren Ergebnisse mit Versuchsdaten verglichen werden. Darüber hinaus kann der Bereich der Umgebungsbedingungen bestimmt werden, für welche eine bestimmter Ansatz realistisch ist, woraus dann die Gültigkeitsgrenzen der verschiedenen Ansätze abgeleitet werden können. Es wird gezeigt, daß keiner der Ansätze ausreichend für ein allgemeines Reifbildungsmodell ist. Als ein Ergebnis wird eine neue umfassendere Methode zur Berechnung der Wärmeleitfähigkeit des Reifs sowohl auf theoretischer als auch experimenteller Grundlage entwickelt.

ОБОБЩЕННАЯ ЗАВИСИМОСТЬ ДЛЯ РАСЧЕТА КОЭФФИЦИЕНТА ТЕПЛОПРОВОДНОСТИ ОБРАЗОВАННОГО ИЗ ВОДЫ ИНЕЯ

Аннотация—В последние годы вновь привлекли к себе внимание исследования образования инея. Существенным для разработки модели процесса оказался вывод коэффициента теплопроводности инея. Этому вопросу и посвящена предлагаемая работа. Теплопроводность слоя инея играет важную роль для определения его структуры и скорости образования. Ряд авторов рассматривал проблему расчета коэффициента теплопроводности. В данной работе выполнена проверка различных методик, которые применялись этими авторами, путем анализа использованных ими допущений. Рассматриваются все возможные механизмы теплопереноса внутри слоя с целью выяснения вопроса, какие из процессов являются важными, а какими можно без ущерба пренебречь. На основании этого можно провести оценку различных использованных ранее методик и полученные результаты сравнить с экспериментальными данными. Кроме того, можно определить диапазон внешних воздействий, для которых справедлива каждая из методик и тогда определить присущие им ограничения. Показано, что ни одна из них не пригодна для разработки обобщенной модели образования инея. В результате на основе аналитических и экспериментальных данных был предложен новый, более корректный, метод расчета коэффициента теплопроводности инея.